remote sensing

MDPI

Review

A Review of Quantifying pCO_2 in Inland Waters with a Global Perspective: Challenges and Prospects of Implementing Remote Sensing Technology

Zhidan Wen [1], Yingxin Shang [1], Lili Lyu [1], Sijia Li [1], Hui Tao [1] and Kaishan Song [1,2,*]

[1] Northeast Institute of Geography and Agroecology, Chinese Academy of Sciences, Changchun 130102, China; wenzhidan@iga.ac.cn (Z.W.); shangyingxin@iga.ac.cn (Y.S.); lvlili0814@sina.com (L.L.); lisj983@nenu.edu.cn (S.L.); taohui@iga.ac.cn (H.T.)

[2] School of Environment and Planning, Liaocheng University, Liaocheng 252000, China

* Correspondence: songks@neigae.ac.cn

Abstract: The traditional field-based measurements of carbon dioxide (pCO_2) for inland waters are a snapshot of the conditions on a particular site, which might not adequately represent the pCO_2 variation of the entire lake. However, these field measurements can be used in the pCO_2 remote sensing modeling and verification. By focusing on inland waters (including lakes, reservoirs, rivers, and streams), this paper reviews the temporal and spatial variability of pCO_2 based on published data. The results indicate the significant daily and seasonal variations in pCO_2 in lakes. Rivers and streams contain higher pCO_2 than lakes and reservoirs in the same climatic zone, and tropical waters typically exhibit higher pCO_2 than temperate, boreal, and arctic waters. Due to the temporal and spatial variations of pCO_2, it can differ in different inland water types in the same space-time. The estimation of CO_2 fluxes in global inland waters showed large uncertainties with a range of 1.40–3.28 Pg C y^{-1}. This paper also reviews existing remote sensing models/algorithms used for estimating pCO_2 in sea and coastal waters and presents some perspectives and challenges of pCO_2 estimation in inland waters using remote sensing for future studies. To overcome the uncertainties of pCO_2 and CO_2 emissions from inland waters at the global scale, more reliable and universal pCO_2 remote sensing models/algorithms will be needed for mapping the long-term and large-scale pCO_2 variations for inland waters. The development of inverse models based on dissolved biogeochemical processes and the machine learning algorithm based on measurement data might be more applicable over longer periods and across larger spatial scales. In addition, it should be noted that the remote sensing-retrieved pCO_2/the CO_2 concentration values are the instantaneous values at the satellite transit time. A major technical challenge is in the methodology to transform the retrieved pCO_2 values on time scales from instant to days/months, which will need further investigations. Understanding the interrelated control and influence processes closely related to pCO_2 in the inland waters (including the biological activities, physical mixing, a thermodynamic process, and the air–water gas exchange) is the key to achieving remote sensing models/algorithms of pCO_2 in inland waters. This review should be useful for a general understanding of the role of inland waters in the global carbon cycle.

Keywords: pCO_2; remote sensing; satellites; inland waters; CO_2 flux

Citation: Wen, Z.; Shang, Y.; Lyu, L.; Li, S.; Tao, H.; Song, K. A Review of Quantifying pCO_2 in Inland Waters with a Global Perspective: Challenges and Prospects of Implementing Remote Sensing Technology. *Remote Sens.* **2021**, *13*, 4916. https://doi.org/10.3390/rs13234916

Academic Editor: Pradeep Wagle

Received: 17 October 2021
Accepted: 30 November 2021
Published: 3 December 2021

1. Introduction

Inland waters are an important component of the global carbon cycle. They function as active pipes to transport and transform a large quantity of naturally and anthropogenically derived carbon [1–4]. They serve as passive conduits from soil to sea and also divert carbon to the atmosphere and sediment sink. Carbon exchange occurs through the vertical interactions between inland waters and the atmosphere, often in the form of greenhouse gases (GHGs). The globally averaged surface temperature (combining land and ocean) has increased by approximately 1.0 °C (0.8–1.2 °C) above the pre-industrial levels [5].

Rising emission of natural and anthropogenic GHGs is highly likely to be the dominant cause of the observed warming since the mid-20th century [6]. Carbon dioxide (CO_2) in the atmosphere is the most important GHG because it can enhance the greenhouse effect, with a contribution rate of 60%. A global CO_2 emission survey on inland waters indicated that 95% of the 6708 streams and rivers have a median partial pressure of carbon dioxide (pCO_2) greater than the atmospheric value, and 7939 lakes and reservoirs are supersaturated [3]. The CO_2 flux released by inland waters is of the same order of magnitude as land–atmosphere and land–ocean net carbon exchanges. Hence, long-term monitoring of pCO_2 and CO_2 emissions from inland waters is essential for quantifying and understanding how inland waters contribute to the global carbon cycle [7–9].

The response of regional inland waters to global change has attracted the attention of the international research community [6]. Over the past decade, most of the research efforts have been on refining CO_2 flux estimation at the regional and global scales [3,10–13]. Nevertheless, the quantification of the pCO_2 in inland waters is also important for accurately estimating CO_2 flux in the water–atmosphere interface and understanding the role of CO_2 in inland waters in the Earth's carbon budget. Some studies reported about the significant spatial and temporal variations of the pCO_2 in lakes and rivers [13–17] and the strong influence of ambient environment and river discharge on the pCO_2 of inland waters [18–20]. However, the current pCO_2 data of inland waters remain uncertain due to the large discrepancy of pCO_2 in the global inland waters. Moreover, the variation in CO_2 flux estimation to the atmosphere stems not only from the limited spatiotemporal data availability, but also from various methods in an un-unified pCO_2 estimation approach [12,21,22]. The common methods include the direct measurement of in situ pCO_2 using an air-flushing equilibrator connected to an infrared photoacoustic gas analyzer [23,24]; the underway pCO_2 system [25]; the underwater sensors, e.g., C-Sense^{TM}, HydroC^{TM}-CO_2, and Franatech CO_2-sensor [25,26]; calculation of pCO_2 based on in situ pH, total alkalinity, water temperature, and salinity values of inland waters [27]; and estimation of pCO_2 based on the dissolved CO_2 concentration in the water [28]. There is a lack of an effective and generalized method to characterize the spatial and temporal dynamics of pCO_2 in detail, particularly in some regions with a large freshwater surface area and regions sensitive to climate change [28,29]. According to climate model projections, extreme climatic events (e.g., rainfall and flood) would increase in some regions [30,31]. Some studies showed that intense rainfall events and floods could modify the water–atmosphere exchange of CO_2 [32–34]. It is necessary to develop a common method to estimate pCO_2, which covers long-term records and large spatial coverage, so that we could better illustrate the potential impact of such events on pCO_2 and accurately quantify CO_2 flux and the role of inland waters in the global carbon cycle. Over the past two decades, remote sensing of pCO_2 in the water environment has received much attention due to its unique advantages against the traditional field-based technologies [35]. In addition, this method has the ability to achieve the simultaneous observation and comparison of pCO_2 values in different waters and different times over the same location. The assessment of pCO_2 variations based on multi-source remote sensing data has contributed greatly to the accurate quantification of CO_2 flux in the atmosphere–water interface at high-spatiotemporal resolution in the ocean and coastal waters [36–39], while a similar attempt has also been conducted in the inland waters [11,13,40,41].

The statement is strengthened by the fact that inland waters function as important elements in the global carbon balance despite the smaller overall size relative to the terrestrial ecosystem [42–44]. In this paper, we aim to summarize and discuss the temporal and spatial variability of pCO_2 in inland waters, especially in different water types based on data gathered by Aufdenkampe et al. (2011). We summarize the current state of CO_2 fluxes in inland waters and compare them in different water types and climatic zones. A key open question is the low accuracy of long-term monitoring of pCO_2 in inland waters, and the fact that pCO_2 in inland waters can vary with climate conditions and water types. It also varies seasonally and interannually. Therefore, we analyzed the current pCO_2 remote sensing method in marine and coastal waters at the global scale and put forward the challenges and prospects of using remote sensing to estimate pCO_2 in inland waters.

2. General Background and Motivation of pCO_2 Remote Sensing

2.1. Spatio-Temporal Variability of pCO_2 in Inland Waters

The process of CO_2 exchange in the atmosphere–water system is regulated by the climate and watershed characteristics; meanwhile, the estimation of CO_2 evasion should consider the daily variability of pCO_2. At present, there are limited data that characterize the connection between CO_2 flux and the daily course and variation of pCO_2 in inland waters [16]. Improving the understanding of the daily variation of pCO_2 is a critical step to reduce uncertainties in CO_2 flux estimations for inland waters. Significant daily variation in pCO_2 has been measured in University Lake, a shallow, subtropical, eutrophic lake located in Louisiana, USA, with a consistently declining trend of pCO_2 from early mornings to late afternoons [15,16] (Figure 1). The daily variation in pCO_2 was also observed in stratified water bodies, with a strong relation to the diurnal cycles of metabolic activity [45], while pCO_2 in an unproductive lake in Northern Sweden was found to have low daily variation during summer [46]. In the daytime, pCO_2 dynamics are primarily driven by aquatic metabolism in a eutrophic lake and are associated with the lake's primary and secondary production [16]. Elevated primary production during algal's growing season in a eutrophic lake can draw down CO_2 levels in water. Previous studies showed that algal blooms can reduce carbon emissions to the atmosphere, but algal decomposition could release a large amount of CO_2 [47–49]. High algae productivity can turn a lake from a net CO_2 source to a net CO_2 sink to the atmosphere [50]. Furthermore, previous studies confirmed a close correlation between daily changes of pCO_2 and solar radiation, water temperature, and the lake trophic status [15,16,45,46,51,52].

The pCO_2 in inland waters often shows significant variability at the seasonal scale [45,46,53]. Relative to other seasons, the surface pCO_2 in summer is generally low due to the strong photosynthesis of phytoplankton in lakes and reservoirs, which absorb CO_2 in the water column for primary production [54–57]. In addition, the ice-melt period is a critical time window for CO_2 emissions from boreal lakes [9,58,59], because the accumulated CO_2 sealed in ice and sub-ice water can be quickly released to the atmosphere during ice melt. The growing interest in seasonal pCO_2 estimation indicates the need to consider the influence mechanism of pCO_2 in different inland waters. In stratified reservoirs, seasonal variability of pCO_2 is related to the water temperature dynamics and thermal stratification of the water column [45]. In an oligotrophic unproductive lake, seasonal pCO_2 variation could be driven by changing dissolved inorganic carbon and allochthonous organic matter [29,46]. In rivers, pCO_2 always shows a higher value during the rainy season compared with the dry season [53], and the seasonal pCO_2 variations are generally controlled by flows and dissolved oxygen enrichment [53,60].

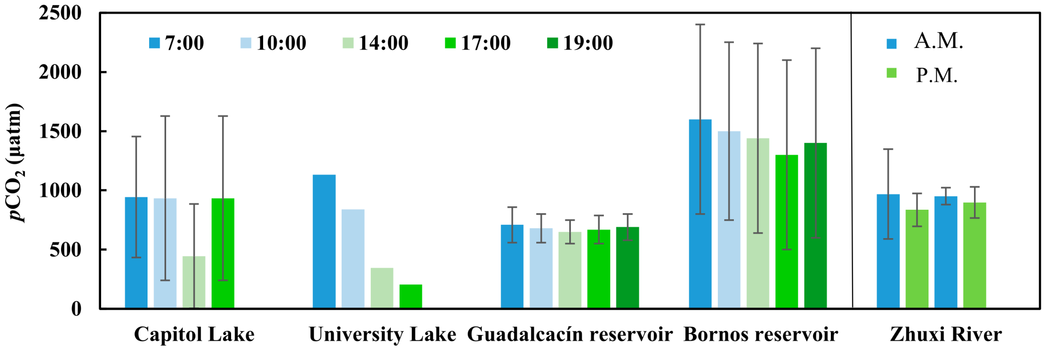

Figure 1. Daily pCO_2 variations in different inland waters; the data were collected from the following references: [15,16,45,61].

Studies across the global inland waters demonstrated that nearly all freshwater bodies are CO_2 supersaturated compared to the atmosphere [62,63]. Measured or calculated pCO_2 values typically vary widely in the global inland waters. In general, according to the statistical analysis of Aufdenkampe et al. (2011), the pCO_2 in rivers and streams is higher than those in lakes and reservoirs in the same climatic zone, and the pCO_2 in tropical waters is higher than those in temperate, boreal, and arctic waters (Figure 2). From published literature, the pCO_2 values of global lakes ranges from 17–65,250 μatm, with a mean value of 1287 ± 41 μatm, and the pCO_2 in Arctic lakes is significantly lower than those in lakes of other climatic zones [20]. The pCO_2 values in reservoirs ranges from 5–10,000 μatm [27,64,65], and CO_2 emissions in reservoirs are correlated to the built age and latitude, with CO_2 emission rates from the tropical Amazon region significantly higher than other climatic zones [65,66]. In addition, reservoirs often exhibit higher mean pCO_2 than lakes in the same region [27,42,63]. The pCO_2 in rivers and streams ranges from 582 μatm to more than 12,000 μatm [44,49]. The riverine pCO_2 at the global scale demonstrates a decreasing trend from low to high latitudes [3,44,65], and a similar trend is also well established with rivers' and streams' order and length in riverine networks [67]. Riverine pCO_2 interacts with aqueous carbon and nutrients and can reach significantly high levels when the level of nutrients in the water is high [61].

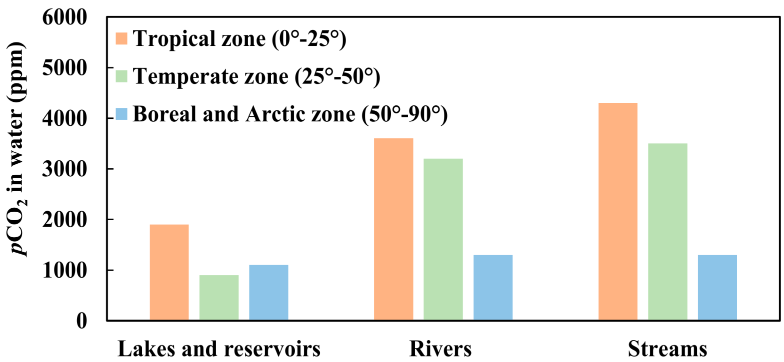

Figure 2. Graphical representation of pCO_2 in different inland waters' zones based on atmospheric circulation; the data were collected from the following article: [65]. The values showed in the figure are median values. The rivers' class and streams' class were calculated by Lehner and Doll's (2004) and Downing's (2009) methods [68,69].

2.2. The Current State of CO_2 Fluxes in Inland Waters

Inland waters are widely considered as significant sources of CO_2 to the atmosphere [7,42,63,70–72]. Most studies up-scaled the local or regional CO_2 fluxes' measurements in inland waters to the globe by multiplying an average emission rate by the global area. However, these calculations contained large uncertainties due to the change and inaccurate estimation of global inland waters' surface area and gas transfer rate. For example, the global CO_2 flux from inland waters estimated by Cole et al. (2007) was only 750 Tg y^{-1}, because the data sets used in that estimation merely covered about 5000 individual lakes spanning across the globe, the largest reservoirs in the world (excluding the very small reservoirs), more than 80 of the world's largest rivers, and only the main channels of the rivers. However, the global CO_2 flux from inland waters estimated by Raymond et al. (2013) reached 2100 Tg y^{-1}. That estimation provided a total global surface area of inland waters of 3,620,000 km^2. They combined lakes and reservoirs with streams and rivers, including lakes and reservoirs <3.16 km^2 and the first-order streams. To date, the global CO_2 evasion from inland waters to the atmosphere ranges from 1.40–3.28 Pg C y^{-1} [3,42]. The contributions of inland water CO_2 to atmosphere also vary with regions and water types (Table 1). For example, the inland waters in India and China yielded average CO_2 emissions of 22.0 Tg yr^{-1} [73] and 98 ± 19 Tg yr^{-1} [11], respectively. The total CO_2 emitted by global saline lakes ranges from 110–150 Tg yr^{-1} [72], while that emitted by all German drinking water reservoirs is about 0.44 Tg y^{-1} [74] and that emitted by the lakes and ponds of Florida is roughly 2.0 Tg y^{-1} [70]. Fluxes of greenhouse gases in boreal reservoirs are usually 3–10 times higher than those in natural lakes at their maximum [42]. In addition, the global stream and rivers are also the hotspots of CO_2 efflux [3] and they make a nonnegligible contribution to CO_2 flux from inland waters to the atmosphere that does not correspond to their area proportion in the whole inland waters area. Globally, conservative estimates imply that 26.7–64.4% of total CO_2 emissions from inland waters originate from rivers and streams (Figure 3). In the Amazon basin, CO_2 evasion from streams, rivers, and wetlands of the region could reach as high as 500 Tg y^{-1}, and this value was later revised upward due to CO_2 supersaturation in some small headwater streams [75,76]. In the 2010s, the amounts of CO_2 evasion from streams and rivers in the United States, China, and Africa were 97 $\pm$ 32 Tg C y^{-1} [77], 85.8 $\pm$ 19.4 Tg C y^{-1} [11], and 270–370 Tg C yr^{-1} [78], respectively. In addition, some studies suggested that the contribution of very small ponds (<0.001 km^2) to inland water CO_2 emissions could not be ignored despite their small total surface area of the inland water [79], and some researchers indicated the need of paying attention to the CO_2 emissions from exposed river sediments during drought period [80,81].

Table 1. The global and regional estimate of inland waters' CO2 emission to atmosphere.

Region	Water Type	CO_2 Emission	Ref.
Global	Inland waters	2100 Tg C y^{-1}	[3]
Global	Inland waters	3280 Tg y^{-1}	[82]
Global	Inland waters	750 Tg y^{-1}	[1]
Global	Inland waters	1400 Tg y^{-1}	[42]
Global	Streams and rivers	1800 $\pm$ 250 Tg y^{-1}	[3]
Global	Streams and rivers	560 Tg y^{-1}	[65]
Global	Streams and rivers	650 Tg y^{-1}	[44]
Global	Lakes and reservoirs	320 + 520, −260 Tg y^{-1}	[3]
Global	Lakes and impoundments	810 Tg y^{-1}	[42]
Global	Lakes and impoundments	245–527 Tg y^{-1}	[21]
Global	Lakes and reservoirs	640 Tg y^{-1}	[65]
Global	Lakes	530 Tg y^{-1}	[72]
Global	Saline lakes	110–150 Tg y^{-1}	[72]
Global	Reservoirs	280 Tg y^{-1}	[1]
Global	Reservoirs	273 Tg y^{-1}	[62]
Global	Hydroelectric reservoirs	48 Tg y^{-1}	[66]
Boreal and arctic region	Inland waters	150 Tg yr^{-1}	[65]
Boreal region	Lakes	189 Tg yr^{-1}	[13]
Boreal and arctic region	Lakes and reservoirs	110 Tg yr^{-1}	[65]
Africa	Rivers	270–370 Tg yr^{-1}	[78]
Amazon	Reservoirs	8 Tg yr^{-1}	[66]
Boreal region	Reservoirs	6	[66]
Temperate	Reservoirs	5	[66]
Tropical	Reservoirs	37	[66]
Amazon	The lower river	480 Tg yr^{-1}	[83]
Amazon	Streams, rivers, and wetlands	500 Tg y^{-1}	[75,83]

Table 1. *Cont.*

Region	Water Type	CO_2 Emission	Ref.
Germany	Drinking water reservoirs	0.44 Tg y^{-1}	[74]
United States	Streams and rivers	97 $\pm$ 32 Tg y^{-1}	[77]
Florida	Lakes and ponds	2.0 Tg y^{-1}	[70]
China	Inland waters	66–136 Tg yr^{-1}	[11]
China	Hydroelectric reservoirs	29.6 Tg y^{-1}	[43]
China	Streams and rivers	19.4 Tg yr^{-1}	[11]
China	Lakes and reservoirs	12.1 Tg yr^{-1}	[11]
China	Lakes and reservoirs	25.15 Tg yr^{-1}	[12]
India	Inland waters	22.0 Tg y^{-1}	[73]

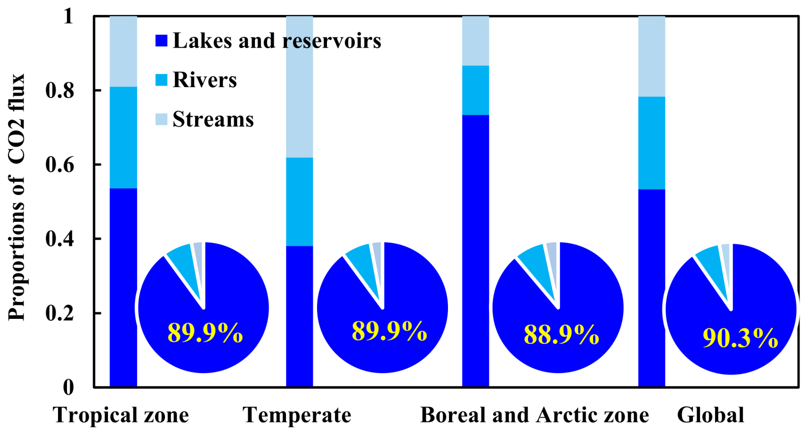

Figure 3. The proportions of inland water CO_2 flux in different climatic zones; the data were collected from the following article: [65]. The pie chart denotes the area proportions of different inland waters type.

Furthermore, previous studies on long-term monitoring of the CO_2 flux in inland waters revealed that some lakes switched between acting as a CO_2 source and sink [7–9]. This highlights that it is important to fully understand the mechanisms and influence factors controlling CO_2 evasion. The increase of CO_2 flux in the atmosphere–lake system is generally considered synchronous to the decrease in photosynthetic activity of plankton [51]. CO_2 supersaturation often exists in lakes when the respiration exceeds photosynthesis in lakes [56,84]. Beyond that, the inputs of dissolved carbon from carbonate weathering in lake and watershed should also be considered for the CO_2 supersaturation [20,63]. The lake's size, trophic status, ice presence/absence, algal blooms, and salinity all have important implications on CO_2 emissions [21,71,72,85–91]. Algal blooms in some lakes could reduce carbon emissions, while the algal-derived organic carbon during the algae degradation process could increase the subsequent CO_2 production [47,48,50,92]. Saline lakes could raise the total CO_2 emissions to the atmosphere more than freshwater lakes [72]. Eutrophication with the enhanced organic matter decay and biological activity could increase lacustrine CO_2 emissions [27,49,85]. Understanding the source of inland water CO_2, the influence of diel and seasonal pCO_2 changes on CO_2 outgassing estimation, and the exchange mechanism of carbon between different ecosystems is important for the accurate estimation of CO_2 evasion in inland waters globally, which has a major impact on the global carbon biogeochemical cycles.

3. Studies on Remote Sensing of pCO_2

According to existing theoretical analysis and research results, pCO_2 in water surface cannot be directly derived from satellite radiance. It is mostly an indirect measurement that requires the estimation of other variables first. The remote sensing of pCO_2 in water surface requires some environmental variables related to the pCO_2 controlling processes as indicators (e.g., water surface temperature (T), water salinity (S), plankton concentration (Chla), colored dissolved organic matter (CDOM), mixed layer depth). There is also some directly remote sensing research of the dissolved CO_2 concentration or pCO_2 by developing the estimation model based on satellite imagery-derived products. At present, while remote sensing technology has been successfully applied for the estimation of pCO_2 in water surface, most of these studies focused on ocean and coastal waters.

3.1. Remote Sensing Estimating pCO$_2$ in Marine and Coastal Waters

Research on remote sensing of pCO_2 in sea and coastal waters has received much attention in recent years. It is useful for the accurate description of the spatial-temporal heterogeneity of sea-surface CO_2 flux and for quantifying the ocean's role in the global carbon cycle [39,93,94]. Moderate-Resolution Imaging Spectroradiometer (MODIS) imagery and MODIS-derived products are more commonly used in these pCO_2 remote sensing inversion processes [38,94–96]. Related studies using statistical approaches and machine learning techniques have been conducted in many seas and coastal sites (Figure 4), e.g., the Gulf of Mexico [36,97,98], East China Sea [99,100], Caribbean Sea [94], Bering Sea [39], and West Florida Shelf [93]. In general, the empirical algorithms (e.g., linear or multiple regression relationships) and machine learning approaches can work reasonably well with good pCO_2 inversion results in the specified areas [36,38,98]. However, pCO_2 in the open ocean and coastal regions often exhibits a profound spatiotemporal heterogeneity and is controlled by multiple factors. Due to incomprehension of pCO_2 variability mechanisms, these empirical algorithms can only function reliably for areas with available in situ pCO_2 data. Thus, more complex semi-analysis algorithms, combined with the analysis of the main mechanisms causing pCO_2 variability, have been developed in different coastal waters and seas, such as the first implementation of a mechanistic semi-analytic algorithm (MeSAA) in the East China Sea [39,97,100]. A satellite-based semi-mechanistic model was developed for the river-dominated Louisiana Continental Shelf [101], while a nonlinear semi-empirical model with the self-organizing map (SOM) was implemented in the Pacific coast of central North America [102]. Nevertheless, the existing semi-analytical algorithms also have limited applicability in different regions, primarily because of the difficulty in parameterizing and standardizing the physicochemical and biological influence on pCO_2 in sea and coastal waters. In the process of constructing the pCO_2 remote sensing algorithm/model, it is important to choose and develop accurate quantitative expressions relating satellite-derived parameters based on controlling mechanistic analysis, which can assist to better implement remote sensing of pCO_2 in the similar oceanic conditions.

According to a survey of literature, the net sea–air CO_2 flux of the global ocean is approximately 1.4 Pg y^{-1} [103], and this value is subjected to large uncertainty. The air–sea CO_2 fluxes are different depending on the latitudinal and ecosystem diversity of the coastal ocean (particularly near-shore systems). The physical-biogeochemical distinction (including ocean-dominated margin and river-dominated ocean margin) has significant influence on the sources'/sinks' role of coastal waters [104]. In addition, the marginal seas at high and temperate latitudes often act as sinks of atmospheric CO_2; at subtropical and tropical regions, the marginal seas in these two climatic zones act as sources of atmospheric CO_2 [105]. When integrating CO_2 fluxes in the coastal ocean at the global scale, the diversity, latitudes, and seasonal biological effect on ecosystems should be fully considered.

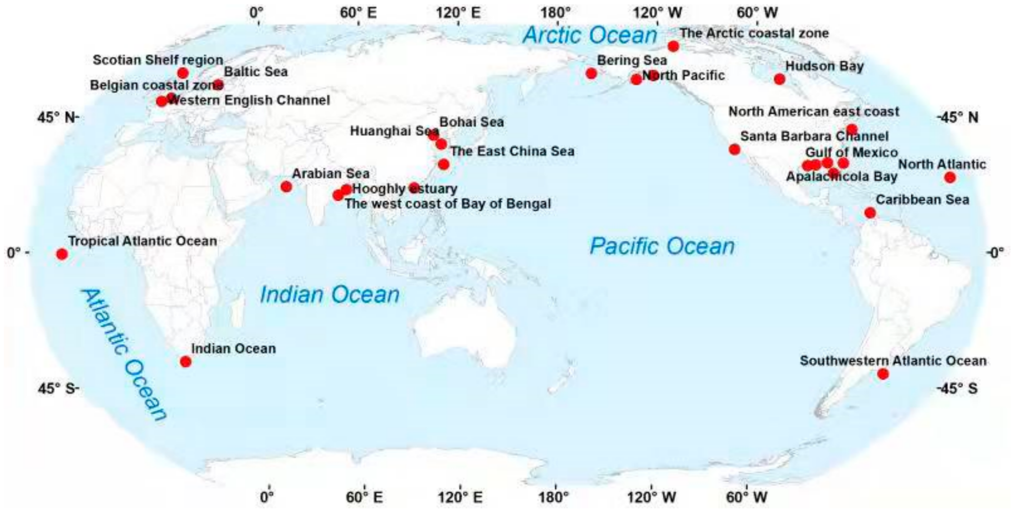

Figure 4. Locations of published works on remote sensing of the surface pCO_2 in sea and coastal waters.

3.2. Remote Sensing of pCO_2 and CO_2 Fluxes for Inland Waters

Typically, inland waters are characterized by the supersaturated, dissolved CO_2 concentrations. However, there are huge differences in optical properties, physicochemical environments, trophic status, and circulation of materials between inland waters and ocean/coastal waters [11,13,40,41]. Some effective remote sensing algorithms and models for pCO_2 in ocean/coastal waters cannot be used directly for that in inland waters. Considering the influencing factors and mechanisms of surface pCO_2 in inland waters, some remote sensing algorithms for pCO_2 in inland waters have been developed based on the relationship between pCO_2 and the retrieved water biogeochemical and optical parameters, e.g., chromophoric dissolved organic matter (CDOM) optical property, algal productivity, and water surface temperature [41]. Earlier studies demonstrated that the temporal and spatial distributions of pCO_2 in inland waters often exhibited high heterogeneity, which resulted in a large uncertainty in lake CO_2 flux calculations. Satellite observations of pCO_2 in inland waters could achieve a relatively high frequency and continuous, large-scale, and long-term data compared to field surveys. There are growing studies in this area in recent years despite a small number of published works. Combining with a high-resolution (25-m resolution), stream network map based on remote sensing, a Random Forest model was applied to predict the stream pCO_2 with an average of 1134 µatm (range: 154–8174 µatm) in Denmark, Sweden, and Finland [106]. Estimations of inland waters' CO_2 emissions have been realized in relation to terrestrial net primary production, which can be obtained from a global data set based on remote sensing, such as in a temperate stream network [107] and in boreal lakes [13]. More recently, optical indicators generated from satellite-derived variables have been utilized to estimate pCO_2 indirectly in some rivers and lakes based on the strong relationship between them, such as CDOM optical properties used in the Lower Amazon River [31] and a turbidity index used in the Swedish lakes Mälaren and Tämnaren [30]. Nevertheless, the direct application of the long-term satellite products to estimate pCO_2 or dissolve CO_2 in inland waters is still in its infancy. The long-term series mapping of dissolved CO_2 pattern based on the remote sensing technology was conducted in Lake Taihu, China, which developed a dissolved CO_2 estimation model based on MODIS-derived products. It was applied to perform the spatiotemporal distribution analysis of dissolved CO_2 concentrations from 2003 to 2018 [22]. MERIS products have also been used to estimate lake pCO_2 [40].

When using long-term remote sensing imagery to directly estimate the CO_2 concentration or pCO_2 in waters or retrieving pCO_2 in water from some relevant environmental remote sensing indicators based on stable relationship [38,41,101], it should be noted that the retrieved CO_2 concentration or pCO_2 values are the instantaneous value at the satellite transit time. The previous studies showed some pronounced changes in the CO_2 concentration over a day and seasons [15,22,52]. To achieve the transformation of retrieved pCO_2 values from an instant to hours/days, some researchers have established the relationship between instantaneous lake CO_2 concentration/pCO_2 at the regular satellite flyover and the daily/weekly mean value [15,22,45] by using the satellite estimation results to extrapolate the daily/weekly CO_2 mean values. In addition, combined with the in situ measured values of the diurnal pCO_2 variation and seasonal pCO_2 variation in a lake, we could realize the conversion of the daily value to the seasonal mean value of the lake's CO_2 through cross verification between different sensors with different time resolutions. More observations and additional efforts would be needed to achieve them in the further studies.

In fact, researchers have a full understanding of biogeochemical mechanism of CO_2 generation and consumption in inland waters. Most of the determining and influence factors of pCO_2 or dissolved CO_2 in different inland waters have been elucidated. Some of these factors can be derived from satellite data, e.g., lake surface temperature, chlorophyll-a concentration, latitude, dissolved organic carbon (DOC), and solar radiation absorption. Therefore, in principle, it is possible to identify the spatiotemporal distribution of pCO_2 in a specific lake or river using the satellite-derived variables and realize the long-term estimations. However, the accuracy and universality of the prediction models should be developed and evaluated as a priority in the large-scale estimation. Nevertheless, it is known that the relationships in the prediction models can vary among different lakes and lake regions, which is the current challenge of the pCO_2 remote sensing in inland waters [22,40,41,45,47,100,101,108,109]. Due to the great influence of outside source input, the geochemical processes of inland lakes can show strong spatial heterogeneity, and the influence factors of the pCO_2 in surface water are often coupled together. This leads to the unstable, non-universal relationship between pCO_2 and its indicators among different lakes and lake regions and the large uncertainties from such extrapolations. Consequently, the development of the inverse models based on dissolved biogeochemical processes and the machine learning algorithm based on lots of measurement data may have better applicability over longer periods and across larger spatial scales.

4. Challenges and Limitations of pCO_2 Remote Sensing Algorithms

As presented in this review, there are still many uncertainties about the pCO_2 dynamics of inland waters affected by human activities and climatic change. Due to the variations of pCO_2 in surface water, a significant challenge exists in the quantification of regional air–water CO_2 flux. Satellite remote sensing has been successfully implemented in the synoptic estimation of oceanic surface pCO_2, with its unique advantages of spatiotemporal resolution and coverage. Moreover, recent studies have revealed the presence of four interrelated processes closely related to water surface pCO_2, i.e., biological activities, physical mixing, a thermodynamic process, and the air–water gas exchange. In principle, understanding these control processes of pCO_2 in the inland waters and unearthing the environmental variables linking to these processes, which can be derived from satellite data, are the key to successfully achieving remote sensing of pCO_2 in inland waters. In addition, a longstanding challenge to upscaling based on environmental variables to remote sensing pCO_2 at the larger scale is the limited availability of spatially explicit data sets on inland water characteristics, such as the seasonal fluctuations of area and the ephemeral and intermittent water occurrence.

Some tentative studies have used remote sensing data to estimate pCO_2 or CO_2 flux in inland waters [22,40]. These studies enabled high-resolution mapping of the whole-lake pCO_2 compared to field surveys. The sensors used in the current studies (Landsat, Sentinel-2, MODIS, and MERIS) have provided either high spatiotemporal coverage or sufficient radiometric sensitivity, which can assist reliable estimations of pCO_2 or CO_2 flux in single specific water [80,110,111]. For inland waters (except the optical indicators of surface water used indirectly to estimate pCO_2), direct satellite estimation of pCO_2 or dissolved CO_2 concentrations are required to construct a spatiotemporal map of pCO_2. Additional works will be needed to develop more comprehensive pCO_2 remote algorithms/models in inland waters to improve the long-term and large-scale reliability and universality of models, particularly for inaccessible and remote sites. Considering the working conditions and the validity of remote sensing models, further model evaluation will be needed in other types of lakes or rivers to make it more general than for the particular water bodies for which it was developed. The remote sensing model sensitivity evaluation and model deviation caused by the input variables should be evaluated before model utilization. Furthermore, some typical challenges caused by clouds or algal blooms in satellite images can also reduce model accuracy and increase the uncertainty of pCO_2 estimations.

5. Conclusions

This paper reviewed the temporal and spatial variability of pCO_2 in inland waters (including lakes, reservoirs, rivers, and streams). Existing analyses indicated significant daily variation in pCO_2 in lakes, with a consistently declining trend of pCO_2 from early morning to late afternoon. Meanwhile, pCO_2 values in inland waters also exhibit seasonal variation at a global scale, and the ice-melt period is a critical time window for CO_2 emission from boreal lakes. Overall, tropical waters typically experience higher pCO_2 than temperate, boreal, and arctic waters, while rivers and streams demonstrate higher pCO_2 than in lakes and reservoirs. While rivers and streams occupy a smaller proportion in global inland waters' area, their CO_2 flux contributions to atmosphere are not less than those from the lakes and reservoirs. This review also summarized previous investigations on remote sensing of pCO_2 in sea and coastal waters, which is essential to the accurate description of the spatial-temporal heterogeneity of sea-surface CO_2 flux. Given that the pCO_2 in sea surface cannot be directly derived from satellite radiance, the remote sensing models of sea surface pCO_2 often employ the environmental variables related to the pCO_2 controlling processes as the indicators. The pCO_2 in inland waters is driven by multiple complex factors and mechanisms (e.g., watershed environment, human activities interference, and water quality factors), which are completely different from those in oceans. Despite the studies on the satellite observations of pCO_2 in inland waters increasing rapidly in recent years, only a handful of them have been published. The optical indicators of water (e.g., CDOM optical properties and turbidity index) have been adopted to estimate pCO_2 indirectly in some inland waters. Future research on direct application of long-term satellite products to estimate pCO_2 in inland waters will be needed for mapping the long-term and large-scale pCO_2 distribution patterns. Reliable and generalized pCO_2 remote sensing models/algorithms in inland waters will need to be developed in future studies. In addition, how to achieve the transformation of retrieved instantaneous pCO_2 values to days/months remains a major technical challenge, which is crucial to the accurate estimation of global CO_2 flux from inland waters based on remote sensing technology.

Author Contributions: Conceptualization, Z.W. and K.S.; methodology, Z.W. and Y.S.; formal analysis, Y.S. and L.L.; investigation, Z.W., Y.S., S.L. and H.T.; data curation, L.L.; writing—original draft preparation, Z.W.; writing—review and editing, K.S.; visualization, S.L.; funding acquisition, Z.W., Y.S. and K.S. All authors have read and agreed to the published version of the manuscript.

Funding: This research was jointly supported by the Strategic Priority Research Program of the Chinese Academy of Sciences (XDA28100100); the Youth Innovation Promotion Association of Chinese Academy of Sciences, China (2020234); the Science and Technology Development Project in Jilin, China (20200201054JC); the National Natural Science Foundation of China (42071336, 42001311); the Research instrument and equipment development project of the Chinese Academy of Sciences (YJKYYQ20190044); and the National Earth System Science Data Center, China (www.geodata.cn, accessed on 29 November 2021) .

Institutional Review Board Statement: Not applicable.

Informed Consent Statement: Not applicable.

Data Availability Statement: Not applicable.

Conflicts of Interest: The authors declare no conflict of interest.

References

1. Cole, J.J.; Prairie, Y.T.; Caraco, N.F.; McDowell, W.H.; Tranvik, L.J.; Striegl, R.G.; Duarte, C.M.; Kortelainen, P.; Downing, J.A.; Middelburg, J.J.; et al. Plumbing the global carbon cycle: Integrating inland waters into the terrestrial carbon budget. *Ecosystems* **2007**, *10*, 171–184. [CrossRef]
2. Meybeck, M.; Vörösmarty, C. Global transfer of carbon by rivers. *Glob. Chang. News* **1999**, *37*, 18–19.
3. Raymond, P.A.; Hartmann, J.; Lauerwald, R.; Sobek, S.; McDonald, C.; Hoover, M.; Butman, D.; Striegl, R.; Mayorga, E.; Humborg, C.; et al. Global carbon dioxide emissions from inland waters. *Nature* **2013**, *503*, 355–359. [CrossRef] [PubMed]
4. Tranvik, L.J.; Cole, J.J.; Prairie, Y.T. The study of carbon in inland waters-from isolated ecosystems to players in the global carbon cycle. *Limnol. Oceanogr. Lett.* **2018**, *3*, 41–48. [CrossRef]
5. IPCC. *Global Warming of 1.5 °C. An IPCC Special Report on the Impacts of Global Warming of 1.5 °C above Pre-Industrial Levels and Related Global Greenhouse Gas Emission Pathways, in the Context of Strengthening the Global Response to the Threat of Climate Change, Sustainable Development, and Efforts to Eradicate Poverty*; IPCC: Geneva, Switzerland, 2018.
6. IPCC. *Climate Change 2014: Synthesis Report. Contribution of Working Groups I, II and III to the Fifth Assessment Report of the Intergovernmental Panel on Climate Change*; IPCC: Geneva, Switzerland, 2014; pp. 1–151.
7. Yan, X.; Ma, J.; Li, Z.; Ji, M.; Xu, J.; Xu, X.; Wang, G.; Li, Y. CO_2 dynamic of Lake Donghu highlights the need for long-term monitoring. *Environ. Sci. Pollut. Res. Int.* **2020**, *28*, 10967–10976. [CrossRef]
8. Bogard, M.J.; del Giorgio, P.A. The role of metabolism in modulating CO_2 fluxes in boreal lakes. *Glob. Biogeochem. Cycles* **2016**, *30*, 1509–1525. [CrossRef]
9. Chmiel, H.E.; Hofmann, H.; Sobek, S.; Efremova, T.; Pasche, N. Where does the river end? Drivers of spatiotemporal variability in CO_2 concentration and flux in the inflow area of a large boreal lake. *Limnol. Oceanogr.* **2020**, *65*, 1161–1174. [CrossRef]
10. Raymond, P.A.; Oh, N.-H.; Turner, R.E.; Broussard, W. Anthropogenically enhanced fluxes of water and carbon from the Mississippi River. *Nature* **2008**, *451*, 449–452. [CrossRef] [PubMed]
11. Ran, L.; Butman, D.E.; Battin, T.J.; Yang, X.; Tian, M.; Duvert, C.; Hartmann, J.; Geeraert, N.; Liu, S. Substantial decrease in CO_2 emissions from Chinese inland waters due to global change. *Nat. Commun.* **2021**, *12*, 1730. [CrossRef]
12. Li, S.; Bush, R.T.; Santos, I.R.; Zhang, Q.; Song, K.; Mao, R.; Wen, Z.; Lu, X.X. Large greenhouse gases emissions from China's lakes and reservoirs. *Water Res.* **2018**, *147*, 13–24. [CrossRef]
13. Hastie, A.; Lauerwald, R.; Weyhenmeyer, G.; Sobek, S.; Verpoorter, C.; Regnier, P. CO_2 evasion from boreal lakes: Revised estimate, drivers of spatial variability, and future projections. *Glob. Change Biol.* **2018**, *24*, 711–728. [CrossRef] [PubMed]
14. Han, B.; Meng, X.; Yang, Q.; Wu, R.; Lv, S.; Li, Z.; Wang, X.; Li, Y.; Yu, L. Connections Between Daily Surface Temperature Contrast and CO_2 Flux Over a Tibetan Lake: A Case Study of Ngoring Lake. *J. Geophys. Res.-Atmos.* **2020**, *125*, e2019JD032277. [CrossRef]
15. Xu, Y.J.; Xu, Z.; Yang, R. Rapid daily change in surface water pCO_2 and CO_2 evasion: A case study in a subtropical eutrophic lake in Southern USA. *J. Hydrol.* **2019**, *570*, 486–494. [CrossRef]
16. Yang, R.; Xu, Z.; Liu, S.; Xu, Y.J. Daily $pCO_{(2)}$ and CO_2 flux variations in a subtropical mesotrophic shallow lake. *Water Res.* **2019**, *153*, 29–38. [CrossRef] [PubMed]
17. Ngochera, M.J.; Bootsma, H.A. Spatial and temporal dynamics of $pCO_{(2)}$ and CO_2 flux in tropical Lake Malawi. *Limnol. Oceanogr.* **2020**, *65*, 1594–1607. [CrossRef]
18. Sobek, S.; Algesten, G.; Bergstrom, A.K.; Jansson, M.; Tranvik, L.J. The catchment and climate regulation of $pCO_{(2)}$ in boreal lakes. *Glob. Chang. Biol.* **2003**, *9*, 630–641. [CrossRef]
19. Jones, S.E.; Kratz, T.K.; Chiu, C.-Y.; McMahon, K.D. Influence of typhoons on annual CO_2 flux from a subtropical, humic lake. *Glob. Chang. Biol.* **2009**, *15*, 243–254. [CrossRef]
20. Marce, R.; Obrador, B.; Morgui, J.-A.; Lluis Riera, J.; Lopez, P.; Armengol, J. Carbonate weathering as a driver of CO_2 supersaturation in lakes. *Nat. Geosci.* **2015**, *8*, 107–111. [CrossRef]
21. DelSontro, T.; Beaulieu, J.J.; Downing, J.A. Greenhouse gas emissions from lakes and impoundments: Upscaling in the face of global change. *Limnol. Oceanogr. Lett.* **2018**, *3*, 64–75. [CrossRef] [PubMed]
22. Qi, T.; Xiao, Q.; Cao, Z.; Shen, M.; Ma, J.; Liu, D.; Duan, H. Satellite Estimation of Dissolved Carbon Dioxide Concentrations in China's Lake Taihu. *Environ. Sci. Technol.* **2020**, *54*, 13709–13718. [CrossRef]
23. Frankignoulle, M.; Borges, A.; Biondo, R. A new design of equilibrator to monitor carbon dioxide in highly dynamic and turbid environments. *Water Res.* **2001**, *35*, 1344–1347. [CrossRef]
24. Abril, G.; Richard, S.; Guerin, F. In situ measurements of dissolved gases (CO_2 and CH_4) in a wide range of concentrations in a tropical reservoir using an equilibrator. *Sci. Total Environ.* **2006**, *354*, 246–251. [CrossRef]
25. Zhang, C.; Wang, C.; Ning, C.; Pang, Y. Intercomparison Study of Seawater pCO_2 Measuring Instruments. *Periodical Ocean Univ. China* **2015**, *45*, 80–86.
26. Reiman, J.H.; Xu, Y.J. Dissolved carbon export and CO_2 outgassing from the lower Mississippi River—Implications of future river carbon fluxes. *J. Hydrol.* **2019**, *578*, 124093. [CrossRef]
27. Wen, Z.; Song, K.; Shang, Y.; Fang, C.; Li, L.; Lv, L.; Lv, X.; Chen, L. Carbon dioxide emissions from lakes and reservoirs of China: A regional estimate based on the calculated pCO_2. *Atmos. Environ.* **2017**, *170*, 71–81. [CrossRef]

28. Wen, Z.; Song, K.; Zhao, Y.; Jin, X. Carbon dioxide and methane supersaturation in lakes of semi-humid/semi-arid region, Northeastern China. *Atmos. Environ.* **2016**, *138*, 65–73. [CrossRef]
29. Atilla, N.; McKinley, G.A.; Bennington, V.; Baehr, M.; Urban, N.; DeGrandpre, M.; Desai, A.R.; Wu, C. Observed variability of Lake Superior $pCO_{(2)}$. *Limnol. Oceanogr.* **2011**, *56*, 775–786. [CrossRef]
30. Yamamoto, K.; Sayama, T.; Apip. Impact of climate change on flood inundation in a tropical river basin in Indonesia. *Prog. Earth Planet. Sci.* **2021**, *8*, 5. [CrossRef]
31. Saurav, K.C.; Shrestha, S.; Ninsawat, S.; Chonwattana, S. Predicting flood events in Kathmandu Metropolitan City under climate change and urbanisation. *J. Environ. Manag.* **2021**, *281*, 111894. [CrossRef]
32. Takagaki, N.; Komori, S. Effects of rainfall on mass transfer across the air-water interface. *J. Geophys. Res.-Ocean.* **2007**, *112*. [CrossRef]
33. Macklin, P.A.; Suryaputra, I.G.N.A.; Maher, D.T.; Sidik, F.; Santos, I.R. Carbon dioxide dynamics in a tropical estuary over seasonal and rain-event time scales. *Cont. Shelf Res.* **2020**, *206*, 104196. [CrossRef]
34. Han, G.; Chu, X.; Xing, Q.; Li, D.; Yu, J.; Luo, Y.; Wang, G.; Mao, P.; Rafique, R. Effects of episodic flooding on the net ecosystem CO_2 exchange of a supratidal wetland in the Yellow River Delta. *J. Geophys. Res.-Biogeosci.* **2015**, *120*, 1506–1520. [CrossRef]
35. Lees, K.J.; Quaife, T.; Artz, R.R.E.; Khomik, M.; Clark, J.M. Potential for using remote sensing to estimate carbon fluxes across northern peatlands—A review. *Sci. Total Environ.* **2018**, *615*, 857–874. [CrossRef] [PubMed]
36. Fu, Z.; Hu, L.; Chen, Z.; Zhang, F.; Shi, Z.; Hu, B.; Du, Z.; Liu, R. Estimating spatial and temporal variation in ocean surface pCO_2 in the Gulf of Mexico using remote sensing and machine learning techniques. *Sci. Total Environ.* **2020**, *745*, 140965. [CrossRef]
37. Lafont, S.; Kergoat, L.; Dedieu, G.; Chevillard, A.; Karstens, U.; Kolle, O. Spatial and temporal variability of land CO_2 fluxes estimated with remote sensing and analysis data over western Eurasia. *Tellus Ser. B-Chem. Phys. Meteorol.* **2002**, *54*, 820–833. [CrossRef]
38. Else, B.G.T.; Yackel, J.J.; Papakyriakou, T.N. Application of satellite remote sensing techniques for estimating air-sea CO_2 fluxes in Hudson Bay, Canada during the ice-free season. *Remote Sens. Environ.* **2008**, *112*, 3550–3562. [CrossRef]
39. Song, X.; Bai, Y.; Cai, W.-J.; Chen, C.-T.A.; Pan, D.; He, X.; Zhu, Q. Remote Sensing of Sea Surface $pCO_{(2)}$ in the Bering Sea in Summer Based on a Mechanistic Semi-Analytical Algorithm (MeSAA). *Remote Sens.* **2016**, *8*, 558. [CrossRef]
40. Kutser, T.; Verpoorter, C.; Paavel, B.; Tranvik, L.J. Estimating lake carbon fractions from remote sensing data. *Remote Sens. Environ.* **2015**, *157*, 138–146. [CrossRef]
41. Valerio, A.d.M.; Kampel, M.; Vantrepotte, V.; Ward, N.D.; Sawakuchi, H.O.; Da Silva Less, D.F.; Neu, V.; Cunha, A.; Richey, J. Using CDOM optical properties for estimating DOC concentrations and $pCO_{(2)}$ in the Lower Amazon River. *Opt. Express* **2018**, *26*, A657–A677. [CrossRef]
42. Tranvik, L.J.; Downing, J.A.; Cotner, J.B.; Loiselle, S.A.; Striegl, R.G.; Ballatore, T.J.; Dillon, P.; Finlay, K.; Fortino, K.; Knoll, L.B.; et al. Lakes and reservoirs as regulators of carbon cycling and climate. *Limnol. Oceanogr.* **2009**, *54*, 2298–2314. [CrossRef]
43. Li, S.; Zhang, Q.; Bush, R.T.; Sullivan, L.A. Methane and CO_2 emissions from China's hydroelectric reservoirs: A new quantitative synthesis. *Environ. Sci. Pollut. Res.* **2015**, *22*, 5325–5339. [CrossRef]
44. Lauerwald, R.; Laruelle, G.G.; Hartmann, J.; Ciais, P.; Regnier, P.A.G. Spatial patterns in CO_2 evasion from the global river network. *Glob. Biogeochem. Cycles* **2015**, *29*, 534–554. [CrossRef]
45. Morales-Pineda, M.; Cozar, A.; Laiz, I.; Ubeda, B.; Galvez, J.A. Daily, biweekly, and seasonal temporal scales of $pCO_{(2)}$ variability in two stratified Mediterranean reservoirs. *J. Geophys. Res.-Biogeosci.* **2014**, *119*, 509–520. [CrossRef]
46. Jonsson, A.; Aberg, J.; Jansson, M. Variations in $pCO_{(2)}$ during summer in the surface water of an unproductive lake in northern Sweden. *Tellus Ser. B-Chem. Phys. Meteorol.* **2007**, *59*, 797–803. [CrossRef]
47. Ouyang, Z.; Shao, C.; Chu, H.; Becker, R.; Bridgeman, T.; Stepien, C.A.; John, R.; Chen, J. The Effect of Algal Blooms on Carbon Emissions in Western Lake Erie: An Integration of Remote Sensing and Eddy Covariance Measurements. *Remote Sens.* **2017**, *9*, 44. [CrossRef]
48. Yan, X.; Xu, X.; Wang, M.; Wang, G.; Wu, S.; Li, Z.; Sun, H.; Shi, A.; Yang, Y. Climate warming and cyanobacteria blooms: Looks at their relationships from a new perspective. *Water Res.* **2017**, *125*, 449–457. [CrossRef] [PubMed]
49. Huttunen, J.T.; Alm, J.; Liikanen, A.; Juutinen, S.; Larmola, T.; Hammar, T.; Silvola, J.; Martikainen, P.J. Fluxes of methane, carbon dioxide and nitrous oxide in boreal lakes and potential anthropogenic effects on the aquatic greenhouse gas emissions. *Chemosphere* **2003**, *52*, 609–621. [CrossRef]
50. Hanson, P.C.; Pollard, A.I.; Bade, D.L.; Predick, K.; Carpenter, S.R.; Foley, J.A. A model of carbon evasion and sedimentation in temperate lakes. *Glob. Chang. Biol.* **2004**, *10*, 1285–1298. [CrossRef]
51. Zavoruev, V.V.; Domysheva, V.M.; Pestunov, D.A.; Sakirko, M.V.; Panchenko, M.V. Daily Course of CO_2 Fluxes in the Atmosphere-Water System and Variable Fluorescence of Phytoplankton during the Open-Water Period for Lake Baikal according to Long-Term Measurements. *Dokl. Earth Sci.* **2018**, *479*, 507–510. [CrossRef]
52. Yang, L.-B.; Li, X.-Y.; Yan, W.-J.; Ma, P.; Wang, J.-N. CH4 Concentrations and Emissions from Three Rivers in the Chaohu Lake Watershed in Southeast China. *J. Integr. Agric.* **2012**, *11*, 665–673. [CrossRef]
53. Manaka, T.; Ushie, H.; Araoka, D.; Otani, S.; Inamura, A.; Suzuki, A.; Hossain, H.M.Z.; Kawahata, H. Spatial and Seasonal Variation in Surface Water $pCO_{(2)}$ in the Ganges, Brahmaputra, and Meghna Rivers on the Indian Subcontinent. *Aquat. Geochem.* **2015**, *21*, 437–458. [CrossRef]

54. Wen, Z.; Song, K.; Zhao, Y.; Shao, T.; Li, S. Seasonal Variability of Greenhouse Gas Emissions in the Urban Lakes in Changchun, China. *Environ. Sci.* **2016**, *37*, 102–111.
55. Lu, L.-C.; Liu, C.Q.; Wang, S.L.; Xu, G.; Liu, F. Seasonal Variability of $p(CO_2)$in the Two Karst Reservoirs,Hongfeng and Baihua Lakes in Guizhou Province, China. *Environ. Sci.* **2007**, *28*, 2674–2681.
56. Cole, J.J.; Pace, M.L.; Carpenter, S.R.; Kitchell, J.F. Persistence of net heterotrophy in lakes during nutrient addition and food web manipulations. *Limnol. Oceanogr.* **2000**, *45*, 1718–1730. [CrossRef]
57. Schindler, D.W.; Broecker, W.S.; Brunskill, G.J.; Peng, T.H.; Emerson, S. Atmospheric carbon dioxide: Its role in maintaining phytoplankton standing crops. *Science* **1972**, *177*, 1192. [CrossRef] [PubMed]
58. Denfeld, B.A.; Kortelainen, P.; Rantakari, M.; Sobek, S.; Weyhenmeyer, G.A. Regional Variability and Drivers of Below Ice CO_2 in Boreal and Subarctic Lakes. *Ecosystems* **2016**, *19*, 461–476. [CrossRef]
59. Karlsson, J.; Giesler, R.; Persson, J.; Lundin, E. High emission of carbon dioxide and methane during ice thaw in high latitude lakes. *Geophys. Res. Lett.* **2013**, *40*, 1123–1127. [CrossRef]
60. Zhai, W.; Dai, M. On the seasonal variation of air-sea CO_2 fluxes in the outer Changjiang (Yangtze River) Estuary, East China Sea. *Mar. Chem.* **2009**, *117*, 2–10. [CrossRef]
61. Li, S.; Luo, J.; Wu, D.; Xu, Y.J. Carbon and nutrients as indictors of daily fluctuations of $pCO_{(2)}$ and CO_2 flux in a river draining a rapidly urbanizing area. *Ecol. Indic.* **2019**, *109*, 105821. [CrossRef]
62. St Louis, V.L.; Kelly, C.A.; Duchemin, E.; Rudd, J.W.M.; Rosenberg, D.M. Reservoir surfaces as sources of greenhouse gases to the atmosphere: A Global estimate. *Bioscience* **2000**, *50*, 766–775. [CrossRef]
63. Sobek, S.; Tranvik, L.J.; Cole, J.J. Temperature independence of carbon dioxide supersaturation in global lakes. *Glob. Biogeochem. Cycles* **2005**, *19*, 208. [CrossRef]
64. Roland, F.; Vidal, L.O.; Pacheco, F.S.; Barros, N.O.; Assireu, A.; Ometto, J.P.H.B.; Cimbleris, A.C.P.; Cole, J.J. Variability of carbon dioxide flux from tropical (Cerrado) hydroelectric reservoirs. *Aquat. Sci.* **2010**, *72*, 283–293. [CrossRef]
65. Aufdenkampe, A.K.; Mayorga, E.; Raymond, P.A.; Melack, J.M.; Doney, S.C.; Alin, S.R.; Aalto, R.E.; Yoo, K. Riverine coupling of biogeochemical cycles between land, oceans, and atmosphere. *Front. Ecol. Environ.* **2011**, *9*, 53–60. [CrossRef]
66. Barros, N.; Cole, J.J.; Tranvik, L.J.; Prairie, Y.T.; Bastviken, D.; Huszar, V.L.M.; del Giorgio, P.; Roland, F. Carbon emission from hydroelectric reservoirs linked to reservoir age and latitude. *Nat. Geosci.* **2011**, *4*, 593–596. [CrossRef]
67. Hutchins, R.H.S.; Prairie, Y.T.; del Giorgio, P.A. Large-Scale Landscape Drivers of CO_2, CH_4, DOC, and DIC in Boreal River Networks. *Glob. Biogeochem. Cycles* **2019**, *33*, 125–142. [CrossRef]
68. Downing, J.A. Global limnology: Up-scaling aquatic services and processes to planet Earth. *Verh. Intern. Ver. Limnol.* **2009**, *30*, 1149–1166. [CrossRef]
69. Lehner, B.; Doll, P. Development and validation of a global database of lakes, reservoirs and wetlands. *J. Hydrol.* **2004**, *296*, 1–22. [CrossRef]
70. Lazzarino, J.K.; Bachmann, R.W.; Hoyer, M.V.; Canfield, D.E., Jr. Carbon dioxide supersaturation in Florida lakes. *Hydrobiologia* **2009**, *627*, 169–180. [CrossRef]
71. Kortelainen, P.; Rantakari, M.; Huttunen, J.T.; Mattsson, T.; Alm, J.; Juutinen, S.; Larmola, T.; Silvola, J.; Martikainen, P.J. Sediment respiration and lake trophic state are important predictors of large CO_2 evasion from small boreal lakes. *Glob. Change Biol.* **2006**, *12*, 1554–1567. [CrossRef]
72. Duarte, C.M.; Prairie, Y.T.; Montes, C.; Cole, J.J.; Striegl, R.; Melack, J.; Downing, J.A. CO_2 emissions from saline lakes: A global estimate of a surprisingly large flux. *J. Geophys. Res.-Biogeosci.* **2008**, *113*, 80. [CrossRef]
73. Selvam, B.P.; Natchimuthu, S.; Arunachalam, L.; Bastviken, D. Methane and carbon dioxide emissions from inland waters in India—implications for large scale greenhouse gas balances. *Glob. Chang. Biol.* **2014**, *20*, 3397–3407. [CrossRef] [PubMed]
74. Saidi, H.; Koschorreck, M. CO_2 emissions from German drinking water reservoirs. *Sci. Total Environ.* **2017**, *581*, 10–18. [CrossRef] [PubMed]
75. Richey, J.E.; Melack, J.M.; Aufdenkampe, A.K.; Ballester, V.M.; Hess, L.L. Outgassing from Amazonian rivers and wetlands as a large tropical source of atmospheric CO_2. *Nature* **2002**, *416*, 617–620. [CrossRef] [PubMed]
76. Johnson, M.S.; Lehmann, J.; Riha, S.J.; Krusche, A.V.; Richey, J.E.; Ometto, J.P.H.B.; Couto, E.G. CO_2 efflux from Amazonian headwater streams represents a significant fate for deep soil respiration. *Geophys. Res. Lett.* **2008**, *35*, 141. [CrossRef]
77. Butman, D.; Raymond, P.A. Significant efflux of carbon dioxide from streams and rivers in the United States. *Nat. Geosci.* **2011**, *4*, 839–842. [CrossRef]
78. Borges, A.V.; Darchambeau, F.; Teodoru, C.R.; Marwick, T.R.; Tamooh, F.; Geeraert, N.; Omengo, F.O.; Guérin, F.; Lambert, T.; Morana, C.; et al. Globally significant greenhouse-gas emissions from African inland waters. *Nat. Geosci.* **2015**, *8*, 637–642. [CrossRef]
79. Holgerson, M.A.; Raymond, P.A. Large contribution to inland water CO_2 and CH_4 emissions from very small ponds. *Nat. Geosci.* **2016**, *9*, 222–226. [CrossRef]
80. Mallast, U.; Staniek, M.; Koschorreck, M. Spatial upscaling of $CO_{(2)}$ emissions from exposed river sediments of the Elbe River during an extreme drought. *Ecohydrology* **2020**, *13*, e2216. [CrossRef]
81. Jin, H.; Yoon, T.K.; Lee, S.H.; Kang, H.; Im, J.; Park, J.H. Enhanced greenhouse gas emission from exposed sediments along a hydroelectric reservoir during an extreme drought event. *Environ. Res. Lett.* **2016**, *11*, 124003. [CrossRef]

82. Alkezweeny, A.J. Aircraft measurements of CO_2, O^{-3}, water vapor, aerosol fluxes and, turbulence over Lake Michigan. *Atmosfera* **1996**, *9*, 137–145.
83. Sawakuchi, H.O.; Neu, V.; Ward, N.D.; Barros, M.d.L.C.; Valerio, A.M.; Gagne-Maynard, W.; Cunha, A.C.; Less, D.F.S.; Diniz, J.E.M.; Brito, D.C.; et al. Carbon Dioxide Emissions along the Lower Amazon River. *Front. Mar. Sci.* **2017**, *4*, 76. [CrossRef]
84. Duarte, C.M.; Prairie, Y.T. Prevalence of heterotrophy and atmospheric CO_2 emissions from aquatic ecosystems. *Ecosystems* **2005**, *8*, 862–870. [CrossRef]
85. Andrade, C.; Cruz, J.V.; Viveiros, F.; Coutinho, R. Diffuse CO_2 emissions from Sete Cidades volcanic lake (Sao Miguel Island, Azores): Influence of eutrophication processes. *Environ. Pollut.* **2020**, *268*, 115624. [CrossRef] [PubMed]
86. Finlay, K.; Vogt, R.J.; Bogard, M.J.; Wissel, B.; Tutolo, B.M.; Simpson, G.L.; Leavitt, P.R. Decrease in CO_2 efflux from northern hardwater lakes with increasing atmospheric warming. *Nature* **2015**, *519*, 215–218. [CrossRef] [PubMed]
87. Li, M.L.; Chen, K.L. CO2 Flux from Qinghai Lake Alpine Wetland Ecosystems on Short-Term Warming and Nitrogen Response; In Proceedings of the International Conference on Energy, Environment and Chemical Engineering (ICEECE 2015). Bangkok, Thailand, 25–26 October 2015; pp. 64–67.
88. Yan, X.; Wu, S.; Xu, J.; Xu, X.; Wang, G. Parallelism of Nutrients and $CO_{(2)}$ Dynamics: Evidence Based on Long-Term Data in Taihu Lake. *Bull. Environ. Contam. Toxicol.* **2020**, *105*, 742–749. [CrossRef]
89. Kosten, S.; Roland, F.; Da Motta Marques, D.M.L.; Van Nes, E.H.; Mazzeo, N.; Sternberg, L.d.S.L.; Scheffer, M.; Cole, J.J. Climate-dependent CO_2 emissions from lakes. *Glob. Biogeochem. Cycles* **2010**, *24*, 91. [CrossRef]
90. Bellido, J.L.; Tulonen, T.; Kankaala, P.; Ojala, A. CO_2 and CH_4 fluxes during spring and autumn mixing periods in a boreal lake (Paajarvi, southern Finland). *J. Geophys. Res.-Biogeosci.* **2009**, *114*, 48. [CrossRef]
91. Finlay, K.; Leavitt, P.R.; Wissel, B.; Prairie, Y.T. Regulation of spatial and temporal variability of carbon flux in six hard-water lakes of the northern Great Plains. *Limnol. Oceanogr.* **2009**, *54*, 2553–2564. [CrossRef]
92. Xiao, Q.T.; Duan, H.T.; Qi, T.C.; Hu, Z.H.; Liu, S.D.; Zhang, M.; Lee, X. Environmental investments decreased partial pressure of CO_2 in a small eutrophic urban lake: Evidence from long-term measurements. *Environ. Pollut.* **2020**, *263*, 114433. [CrossRef]
93. Chen, S.; Hu, C.; Byrne, R.H.; Robbins, L.L.; Yang, B. Remote estimation of surface $p\mathrm{CO}_{(2)}$ on the West Florida Shelf. *Cont. Shelf Res.* **2016**, *128*, 10–25. [CrossRef]
94. Olsen, A.; Trinanes, J.A.; Wanninkhof, R. Sea-air flux of CO_2 in the Caribbean Sea estimated using in situ and remote sensing data. *Remote Sens. Environ.* **2004**, *89*, 309–325. [CrossRef]
95. Huang, W.-J.; Cai, W.-J.; Castelao, R.M.; Wang, Y.; Lohrenz, S.E. Effects of a wind-driven cross-shelf large river plume on biological production and CO_2 uptake on the Gulf of Mexico during spring. *Limnol. Oceanogr.* **2013**, *58*, 1727–1735. [CrossRef]
96. Robbins, L.L.; Daly, K.L.; Barbero, L.; Wanninkhof, R.; He, R.; Zong, H.; Lisle, J.T.; Cai, W.J.; Smith, C.G. Spatial and Temporal Variability of $p\mathrm{CO}_{(2)}$, Carbon Fluxes, and Saturation State on the West Florida Shelf. *J. Geophys. Res.-Ocean.* **2018**, *123*, 6174–6188. [CrossRef]
97. Chen, S.; Hu, C.; Cai, W.-J.; Yang, B. Estimating surface $p\mathrm{CO}_{(2)}$ in the northern Gulf of Mexico: Which remote sensing model to use? *Cont. Shelf Res.* **2017**, *151*, 94–110. [CrossRef]
98. Chen, S.; Hu, C.; Barnes, B.B.; Wanninkhof, R.; Cai, W.-J.; Barbero, L.; Pierrot, D. A machine learning approach to estimate surface ocean $p\mathrm{CO}_2$ from satellite measurements. *Remote Sens. Environ.* **2019**, *228*, 203–226. [CrossRef]
99. Lu, H.; Bai, Y.; Chen, X.; Gong, F.; Zhu, Q.; Wang, D. Satellite remote sensing of the aquatic $p\mathrm{CO}_{(2)}$ in the basin of the South China Sea. In Proceedings of the Remote Sensing of the Ocean, Sea Ice, Coastal Waters, and Large Water Regions 2017, Warsaw, Poland, 11–14 September 2017; Volume 10422. [CrossRef]
100. Bai, Y.; Cai, W.-J.; He, X.; Zhai, W.; Pan, D.; Dai, M.; Yu, P. A mechanistic semi-analytical method for remotely sensing sea surface $p\mathrm{CO}_2$ in river-dominated coastal oceans: A case study from the East China Sea. *J. Geophys. Res. Ocean.* **2015**, *120*, 2331–2349. [CrossRef]
101. Le, C.; Gao, Y.; Cai, W.-J.; Lehrter, J.C.; Bai, Y.; Jiang, Z.-P. Estimating summer sea surface $p\mathrm{CO}_{(2)}$ on a river-dominated continental shelf using a satellite-based semi-mechanistic model. *Remote Sens. Environ.* **2019**, *225*, 115–126. [CrossRef]
102. Hales, B.; Strutton, P.G.; Saraceno, M.; Letelier, R.; Takahashi, T.; Feely, R.; Sabine, C.; Chavez, F. Satellite-based prediction of $p\mathrm{CO}_2$ in coastal waters of the eastern North Pacific. *Prog. Oceanogr.* **2012**, *103*, 1–15. [CrossRef]
103. Takahashi, T.; Sutherland, S.C.; Wanninkhof, R.; Sweeney, C.; Feely, R.A.; Chipman, D.W.; Hales, B.; Friederich, G.; Chavez, F.; Sabine, C.; et al. Climatological mean and decadal change in surface ocean $p\mathrm{CO}_{(2)}$, and net sea-air CO_2 flux over the global oceans. *Deep-Sea Res. Part II-Top. Stud. Oceanogr.* **2009**, *56*, 554–577. [CrossRef]
104. Dai, M.; Cao, Z.; Guo, X.; Zhai, W.; Liu, Z.; Yin, Z.; Xu, Y.; Gan, J.; Hu, J.; Du, C. Why are some marginal seas sources of atmospheric CO2? *Geophys. Res. Lett.* **2013**, *40*, 2154–2158. [CrossRef]
105. Borges, A.V.; Delille, B.; Frankignoulle, M. Budgeting sinks and sources of CO_2 in the coastal ocean: Diversity of ecosystems counts. *Geophys. Res. Lett.* **2005**, *32*, 422. [CrossRef]
106. Martinsen, K.T.; Kragh, T.; Sand-Jensen, K. Carbon Dioxide Partial Pressure and Emission Throughout the Scandinavian Stream Network. *Glob. Biogeochem. Cycles* **2020**, *34*, 14. [CrossRef]
107. Magin, K.; Somlai-Haase, C.; Schaefer, R.B.; Lorke, A. Regional-scale lateral carbon transport and CO_2 evasion in temperate stream catchments. *Biogeosciences* **2017**, *14*, 5003–5014. [CrossRef]
108. Valerio, A.M.; Kampel, M.; Ward, N.D.; Sawakuchi, H.O.; Cunha, A.C.; Richey, J.E. CO_2 partial pressure and fluxes in the Amazon River plume using in situ and remote sensing data. *Cont. Shelf Res.* **2021**, *215*, 104348. [CrossRef]

109. Yu, X.; Wang, Y.; Liu, X.; Liu, X. Remote sensing estimation of carbon fractions in the Chinese Yellow River estuary. *Mar. Georesources Geotechnol.* **2018**, *36*, 202–210. [CrossRef]
110. Brandao, I.L.D.; Mannaerts, C.M.; Brandao, I.W.D.; Queiroz, J.C.B.; Verhoef, W.; Saraiva, A.C.F.; Dantas, H.A. Conjunctive use of in situ gas sampling and chromatography with geospatial analysis to estimate greenhouse gas emissions of a large Amazonian hydroelectric reservoir. *Sci. Total Environ.* **2019**, *650*, 394–407. [CrossRef] [PubMed]
111. Sturtevant, C.S.; Oechel, W.C. Spatial variation in landscape-level CO_2 and CH_4 fluxes from arctic coastal tundra: Influence from vegetation, wetness, and the thaw lake cycle. *Glob. Chang. Biol.* **2013**, *19*, 2853–2866. [CrossRef]